Manuscript submitted to: Volume 2, Issue 3, 260-275.

AIMS Energy DOI: 10.3934/energy.2014.3.260

Received date 24 June 2014, Accepted date 22 July 2014, Published date 5 August 2014

Research Article

Wind Turbines Support Techniques during Frequency Drops — Energy Utilization Comparison

Ayman B. Attya [1,*] and T. Hartkopf [2,*]

[1] Renewable Energies Section, Technical University of Darmstadt, Land-Graf Georg Str. 4, 64283 Darmstadt, Germany.

[2] Renewable Energies Section, Technical University of Darmstadt, Darmstadt, Germany.

* **Correspondence:** Email: a.attya83@yahoo.com; uni@harkopfnet.de

Abstract: The supportive role of wind turbines during frequency drops is still not clear enough, although there are many proposed algorithms. Most of the offered techniques make the wind turbine deviates from optimum power generation operation to special operation modes, to guarantee the availability of reasonable power support, when the system suffers frequency deviations. This paper summarizes the most dominant support algorithms and derives wind turbine power curves for each one. It also conducts a comparison from the point of view of wasted energy, with respect to optimum power generation. The authors insure the advantage of a frequency support algorithm, they previously presented, as it achieved lower amounts of wasted energy. This analysis is performed in two locations that are promising candidates for hosting wind farms in Egypt. Additionally, two different types of wind turbines from two different manufacturers are integrated. Matlab and Simulink are the implemented simulation environments.

Keywords: wind turbine; wind energy; frequency drop; frequency support; de-loading

Nomenclature

WF	Wind Farm
WS	Wind Speed
SOs	System Operators
WT	Wind Turbine
MPT	Maximum Power Tracking
KE	Kinetic Energy
WS_R	Rated wind speed of certain wind turbine

P_{op}	Wind turbine output mechanical power
ρ	Air density
A	Rotor area
β	Pitch angle of wind turbine rotor blades
C_p	Wind turbine performance coefficient
λ_o	Optimum tip speed ratio
λ_{High}	Higher tip speed ratio than optimum value
R	Rotor radius
$WS_{cut\text{-}out}$	Wind turbine cut-out wind speed
$WS_{cut\text{-}in}$	Wind turbine cut-in wind speed
DFIG	Double Fed Induction Generator
DF	De-loading Factor
WS_B	Base wind speed in partial de-loaded operation algorithm
WS_{low}	Low wind speed in partial de-loaded operation algorithm
E_{MPT1}	Generated energy by wind turbine based on MPT1 curve
E_{MPT2}	Generated energy by wind turbine based on MPT2 curve
E_{OS}	Generated energy by wind turbine operated using over-speeding algorithm
E_D	Generated energy by wind turbine operated using de-loaded algorithm
E_{PD}	Generated energies by wind turbine operated using partial de-loaded algorithm

1. Introduction

The expectations of wind energy penetration in conventional power networks are very promising. Several circumstances and new givens are forcing the governments and energy companies to find feasible and reliable alternatives to electricity generation using fossil fuels. The European continent is leading this trend, especially; wind farms (WFs) integration, so that conventional plants (e.g. nuclear power stations) are replaced [1]. However, the intermittent nature of wind energy is a huge obstacle for operators and investors. The continuous variations in wind speed (WS) yield certain commitments on WFs owners, such that they must present a forecast for WFs generation within a predefined duration ahead (e.g. one hour or one day). Afterwards, the system operators (SOs) apply financial penalties when the actual WFs generation deviates from these schedules. On the other side, SOs face hard times during fault events, either frequency or voltage dips, because the traditional primary and secondary responses scenarios are not applicable by WFs. As an illustration, in conventional plants (e.g. steam generators), SOs can easily and efficiently control the output active and reactive powers through governors and excitation systems [2]. This returns to the stable and controllable amounts of fossil fuels used to provide steam to the turbine, and in turn the mechanical power running generator shaft. On the contrary, WS is neither controlled nor expected with high accuracy. To overcome such problems, research activities presented several algorithms to make the wind turbines (WTs) and WFs capable of supporting the system, or at least survive during voltage and frequency events [3, 4]. The authors focus on the proposed algorithms, that make WFs able to support the system during frequency excursions [5, 6, 7]. In other words, WFs contribute positively in frequency deviations curtailment, or at least the negative influence of WS intermittency is almost neutralized (i.e. after WFs replace conventional generators). Literature provided different algorithms to guarantee an acceptable amount of supportive active power, which is injected by WFs during

frequency events. To achieve this aim, WTs are not operated based on maximum power tracking (MPT), but other control methods for speed and/or torque. Generally, the stored kinetic energy (KE) in WT plays a pivot role in these algorithms for example, extractable stored KE is converted into fixed amount of supportive active power during frequency drops elimination [5, 8]. The provision of inertial response by DFIG through artificial speed coupling, and its effects on the machine behavior were analyzed in [9]. On the other hand, WT output power and rotational speed are controlled together to provide active power over-production during frequency excursions. The three offered control regions were classified according to WT rotational speed. Meanwhile, pitch angle influence was neutralized by fixing the pitch angle as long as the WS is below its rated value (WS_R) [10].

WT de-loading (some literature calls it "de-rating") technique is highlighted in [11], such that WT output power is reduced by certain percentage; hence the frequency support is insured by the deficit between optimum and de-loaded power values. Proposed method did not cause any reduction in WT rotational speed; on the contrary, over-speeding technique was implemented to de-load the WT output. Further strategy is presented in [12], where pitch angle control is utilized to keep WT output de-loaded to a predetermined reference value below its optimum. An interesting conclusive comparison is offered in [13] between controlling WT as a conventional generator using droop theory from one side to virtual inertia principle on the other side. It also compared between keeping fixed reserve of active power, regardless the actual output, and keeping a variable reserve relative to the actual output through a fixed percentage (the paper called those two techniques "Balance and Delta" respectively).

Completely different point of view rejects any de-loading or reduction in WFs output, but it counts on energy storage mediums as a solution to curtail the influence of wind power generation intermittent nature. Wide range of energy storage facilities are discussed in literature, mainly, hydro pumping stations, batteries' banks and flywheels [14]. The usage of energy storage eliminates any possibility for wind energy wasting; in contrast, more energy amounts are utilized in charging storage mediums, when the WFs' outputs are high enough so that they are rejected by the grid [15]. The word 'rejected' reflects the conditions of load, conventional generation, and WFs' output, where a portion from WFs output is not utilized to maintain the penetration level of wind power under certain threshold. As an explanation, SOs imposes strict margins on instantaneous wind power penetration in generation mix (i.e. WFs contribution in demand feeding should not exceed certain percentage from the overall generation). These restrictions are applied to minimize the expected drawbacks of sporadic nature of wind power especially, in case of sudden faults and events. Nevertheless, economic constrains halt the expansion of storage solutions, especially, batteries. In addition, geographical and technical problems might face hydro pumping storage plants, and fly wheels ratings are limited.

This paper compares between the amounts of wasted energy according to the integrated support technique. The authors have already presented an algorithm which provides competitive support power during excursions [7]. One of the claimed advantages for this algorithm is reducing the amount of wasted energy compared to other techniques. Thus, the authors demonstrate their claim by comparing the amounts of energies wasted in both de-loading techniques, with respect to the amount of generated energy in case of MPT operation.

The next section explains the method used to obtain MPT performance curves by which optimum harvested energy is evaluated. It also highlights the three considered frequency support techniques, and to achieve completeness, brief summary about the support technique offered by

authors is also presented. The second section also explains applied assessment method for generated energy and the investigated case studies. Third section highlights results and draws light on the merits and cons of each technique, and the last section concludes.

2. Materials and Method

2.1. MPT operation:

The WT output power (P_{op}) depends on three variable parameters, markedly, rotational speed, WS and pitch angle as illustrated by (1) (A and ρ stand for rotor swept area and air density respectively). The integration of pitch angle (β) and rotor speed with the aerodynamic properties of WT decides the optimum value of performance coefficient (C_p) whose empirical formula is (2) (i.e. c_1 to c_6, a and b are constants which differ from one WT type to another [16]). Consequently, the optimum tip speed ratio (λ_o), which achieves optimum C_p of each WT type is obtained. The WT rotational speed is adjusted such that C_p is tracking its optimum value all the time. This constrain is fulfilled by adjusting the value of rotational speed continuously to maintain $\lambda = \lambda_o$ at all WSs using (3), where R stands for rotor radius in meters. Figure (1) illustrates the variation of rotational speed, at different WSs, and the corresponding P_{op} in per unit (p.u.). It is worth mentioning that; β is increased gradually as soon as WS exceeds WS_R. Pitch angle avoids P_{op} from violating the ratings of WT generator. In fact, when WS increases beyond the cut-out WS ($WS_{cut\text{-}out}$), WT stops to avoid physical damage [17].

$$P_{op} = 0.5 \cdot \rho \cdot C_P \cdot A \cdot WS^3 \quad (1)$$

$$C_p(\lambda, \beta) = c_1(c_2 / \lambda_i - c_3\beta - c_4)e^{-c_5/\lambda_i} + c_6\lambda_i$$

$$\frac{1}{\lambda_i} = \left(\frac{1}{a\beta} - \frac{b}{\beta_3 + 1}\right) \quad (2)$$

$$\lambda = \frac{R \cdot rotor\ speed}{WS} \quad (3)$$

The question now is how to simulate the estimation of optimum power value at each WS according to MPT operation. This paper represents the two following approaches to obtain WT performance curves fulfilling MPT:

2.1.1. Manufacturer power curve (MPT 1)

The WT fabricating company provides a standard power curve for each WT type where P_{op} at each WS is indicated within the margin between $WS_{cut\text{-}in}$ and $WS_{cut\text{-}out}$. These power values are based on continuous monitoring for WT performance, and they are the average value of several records at the same WS. Power curve data is manipulated into a lookup table with appropriate interpolation method; hence optimum P_{op} is estimated at any WS using interpolation. The most critical region of this curve is between $WS_{cut\text{-}in}$ and WS_R, elsewhere P_{op} is rated (i.e. 1 p.u.) or zero according to WS.

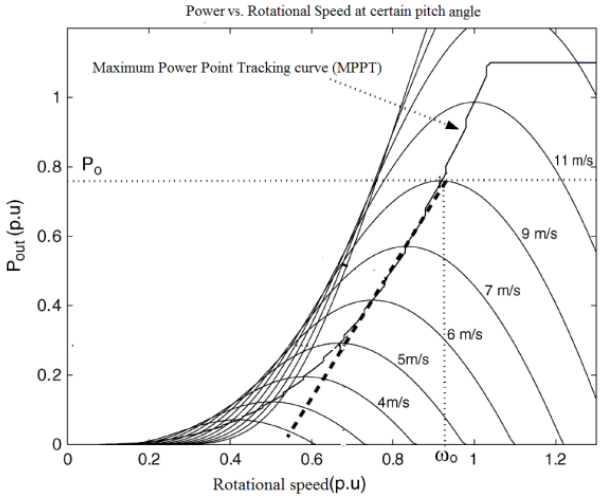

Figure 1. WT output power in MPT operation at different WSs.

2.1.2. Optimum power evaluation using WT model (MPT 2)

This method aims to minimize possible errors in the first one, and it counts mainly on WT model and C_p equation constants. It is well known that variable speed WT has certain range of rotor speeds which is predetermined by the manufacturer. Therefore, the control algorithm driving the WT should not violate these limits to avoid possible loss of synchronism or physical damage. In the proposed algorithm, P_{op} at certain WS is evaluated, using (1 – 3), at all the allowed rotor speeds. Thus, maximum (i.e. optimum) possible P_{op} is determined at each WS starting from $WS_{cut\text{-}in}$ till WS_R. However, the step between two successive WSs (i.e. WS class; for example., WS class = 0.5 m/s thereupon, the examined WSs are; WScut-in + 0.5, WScut-in + 2×0.5, WScut-in + 3×0.5,…., WS_R - 0.5) contributes in the accuracy of the obtained look-up table. In other words, reducing WS class mitigates the role of applied interpolation method, hence error is reduced. Illustrative Figures are provided in results section based on the considered case studies.

It should be highlighted that applying MPT algorithm makes the WT incapable of providing any active power support during frequency excursions, except with the integration of energy storage mediums. However, there still major economic obstacles, which halt the spreading of energy storage techniques to act as system saver during frequency deviations [18].

2.2. Frequency Support techniques

This section explains briefly the WT operation in over-speeding, de-loading and the proposed innovative support technique (it will be called from now on "partial de-loading"). In addition, it explicates the same method that is previously used to construct performance curves of WT in normal operation, but according to the investigated support algorithms.

2.2.1. Over-speeding operation

As mentioned earlier, contribution of WT in frequency drop curtailment count on the amount of stored KE in its rotating parts. Thus, some support techniques aim to increase the amount of stored

and extractable KE. The authors proposed an algorithm which controls the extractable KE by increasing WT rotor speed above its optimum value [5]. Offered algorithm maintains a higher value for λ, hence rotor speed increases, and then the available KE is enlarged. In particular, new value of λ is called λ_{High}, which is more than λ_o by 15 % in this research work. In sequence, λ_{High} is used to evaluate rotor speed at each WS using (4). Afterwards, the three parameters, namely, WS, rotor speed and β are used to estimate P_{op} using (1 – 2). It is worth mentioning that, over-speeding is valid only in the range ($WS_{cut\text{-}in} < WS < WS_R$). As an illustration, starting from WS_R, WT operates at its maximum rotor speed, thus it is invalid to over-speed the WT and violate the rotor speed limits. Moreover, the pitch angle in the considered range always equals to zero, because P_{op} doesn't exceed its rated value. Theoretically, the deviation from λ_o will reduce the amount of generated power in normal operation leading to energy losses compared to MPT.

$$Rotor\ speed_i = \frac{\lambda_{High} \cdot WS_i}{R} \qquad (4)$$
$$\lambda_{High} = 1.15 \times \lambda_o$$

2.2.2. Continuous de-loading operation

WT is operated such that P_{op} is less than the optimum available power all the time. Thus, the deficit between the actual output power, and the optimum one is considered as a strategic reserve to support the system during frequency deviations. As mentioned in the first section; de-loading could be applied by two methods:

- Running the WT at rotational speed higher than the optimum speed (i.e. note that the optimum speed is the speed that leads to $\lambda = \lambda_o$). This method is called WT over-speeding which is valid only for variable speed WTs (e.g. DFIG and Fully rated synchronous generator)
- Activating pitch control at all WSs so that P_{op} is reduced based on the implied pitch angle. This technique is applicable for any WT equipped with pitch angle controls. However, pitching is a slower alternative due to mechanical response of servo motors controlling blades feathering [17].

In both methods a predefined de-loading factor (D_F) is selected by SOs according to their required contribution of WFs in frequency drops mitigation. D_F numerical value is adjusted based on several givens including the level of WFs penetration in system and the history of frequency excursions in the system. Moreover, it is not necessary that all WFs have the same D_F, but it counts on the number and the nameplate ratings of WTs inside each WF. In this paper, it is assumed that D_F equals 15 %, and the minor differences between the two methods are ignored (i.e. WT de-loaded power is the same in both methods).

2.2.3. Partial de-loading algorithm

The major merits and uniqueness of this algorithm lie in three points; 1) it is adapted with WT and WS conditions in the WF location, 2) the de-loading is activated only within certain range of WS which is determined based on certain procedure, 3) its capability to handle WS drops, which intersect with frequency events, reducing the negative impact of WS sudden dips. The first step is to evaluate the pivot three parameters of proposed algorithm, namely, 1) base rotational speed, 2) base WS (WS_B) and 3) low WS (WS_{low}) [7]. The evaluation of base rotational speed counts on obtaining P_{op} array of

the WT type, installed in the WF, at the annual average WS in this location for the whole range of rotational speeds. Thus, the rotational speed yielding the highest P_{op} is selected as base value. Likewise, the P_{op} arrays at base rotational speed are obtained at wide spectrum of WSs; WS at which, P_{op} is within the range of 0.6 to 0.7 p.u. (with respect to nameplate rating) is selected as WS_B.

Finally, WS_{low} is found to be 70 % from WS_B according to extensive experiments. The proposed algorithm operates WT in de-loaded operation within the WS range (WS_{low} < WS < WS_R). De-loading is implied using pitch angle control. It is worth mentioning that, when WS exceeds WS_B by certain margin, rotor speed is allowed to accelerate above its base value, hence higher P_{op} is supplied, and more energy is harvested. At rated P_{op}, the de-loading is deactivated to utilize all the available wind energy, and support is achieved by overloading the WT generator for a predefined duration. When instantaneous WS drops, KE is extracted from WT rotating parts by fixing the former P_{op}, and decelerating the rotational speed to a new speed that avoids loss of synchronism. In words, de-loading is applied at the following conditions: 1) WS_{low} < WS < WS_R and 2) normal P_{op} is less than 1 p.u. Further details about this algorithm are not prerequisites to perform or comprehend the wasted energy analysis considered in this paper.

2.3. Wasted energy assessment

This subsection explains the method used to estimate the amount of generated energy by WT within certain time span according to a given chronological WS array. Therefore, the amount of wasted energies in the discussed frequency support algorithms, are evaluated and compared. WS chronological arrays in certain locations are the input to the constructed look-up tables to estimate the generated wind power within the required time span. A simplified method is implemented to estimate the generated energies using (5 – 8).

$$E_{MPT1} = \sum_{n=1}^{N} P_{op-MPT1\ n} \cdot t_{WS},\ E_{MPT2} = \sum_{n=1}^{N} P_{op-MPT2\ n} \cdot t_{WS} \tag{5}$$

$$E_{OS} = \sum_{n=1}^{N} P_{op-OS} \cdot t_{WS} \tag{6}$$

$$E_{D} = E_{MPT2} \cdot (1 - \frac{DF}{100}) \tag{7}$$

$$E_{PD} = \sum_{n=1}^{N} P_{op-PD} \cdot t_{WS} \tag{8}$$

E_{MPT1} and E_{MPT2} stand for generated energies within considered time span (T), when the output of WT is predicted based on MPT curves that are explained in Subsections 2.1 and 2.2 respectively. E_{OS}, E_D and E_{PD} stand for the generated energies within T, when WT operates using over-speeding, de-loaded and partial de-loaded strategies respectively. The time step (i.e. time duration between each two successive WSs records) of the available chronological WS array is t_{WS}, and N is the number of WSs records within T.

P_{op} is evaluated based on the performance curves of WT type, and the implemented operation technique. As an illustration, the WS array is an input for a single dimensional look-up table, whose

data is obtained from the WT performance curve. However, the transients occurring during the shift from one WS to the next one are ignored due to their minor impact on the generated energy [19].

In general, the energy is the integration of power during time, and as the time deficit between each two successive WS records is fixed (i.e. t_{WS}), hence the energy produced at each WS_i is equivalent to the product of corresponding P_{op-i} and t_{WS}. Meanwhile, P_{op} is reduced by D_F from MPT2 in continuous de-loading operation as implied in (7). Finally, the amount of wasted energy is calculated with correspondence to E_{MPT2}, for example, the difference between E_{MPT2} and E_D represents the wasted energy due to the application of continuous de-loading method.

2.4. Case studies

To emphasis the impact of WS conditions and WT type on the wasted energy in each operation algorithm; two different locations and two WTs types namely, Gameza-90 2 MW (G-90), and General Electric-77-1.5 MW (GE-77) [16, 19], are involved in the presented analysis. Both WTs are characterized by a medium rated output, moderate size, average costs hence they are widely integrated in many WF. In addition, the GE-77 is almost the only WT whose aerodynamic parameters are identified in the MATLAB Simpower library, meanwhile the aerodynamic parameters of G-90 were previously estimated by the authors in [16]. It is not preferred to imply the analysis on a huge WT (e.g., Nordex 117-2.4 MW), as it will provide an optimistic view about the expected losses due to its aerodynamic characteristics, especially at low WSs. On the other side, highly rated WT (e.g., Enercon 101-3.05 MW) is also avoided, as it will aggravate the expected losses margins.

The two locations are selected from WFs candidate sites according to the Egyptian authority of new and renewable energies, namely, Nabq and Ghareb [20]. These two sites are dissimilar in WS conditions as indicated by table (1), such that Ghareb site is characterized by high annual average WS, in contrast to Nabq location with a lower average. These two locations are selected in Egypt because the fund covering this research is partially directed to investigate the Egyptian wind energy prospects. The available WS data are average WSs recorded every 10 minutes (i.e., t_{WS} = 10 minutes and 52560 WS records/year in each location) with 3 % standard deviation within one complete year (i.e., T = 1 year) at an average height of 75 m. These two WS arrays are implemented to execute the methodology explained in Subsection 2.3. Table (1) highlights the probability of occurrence of the main WS categories, which are defined in table (2), in the two sites during one year. In table (1), 'max.' refers to the maximum recorded WS in mentioned site in m/s, and categories occurrence probabilities are in percentages. Major technical specifications of both WTs are mentioned in table (3) and figure (2) displays their MPT 1. The generated energies from the two WTs are estimated to judge the amount of wasted energy in continuous and partial de-loading techniques.

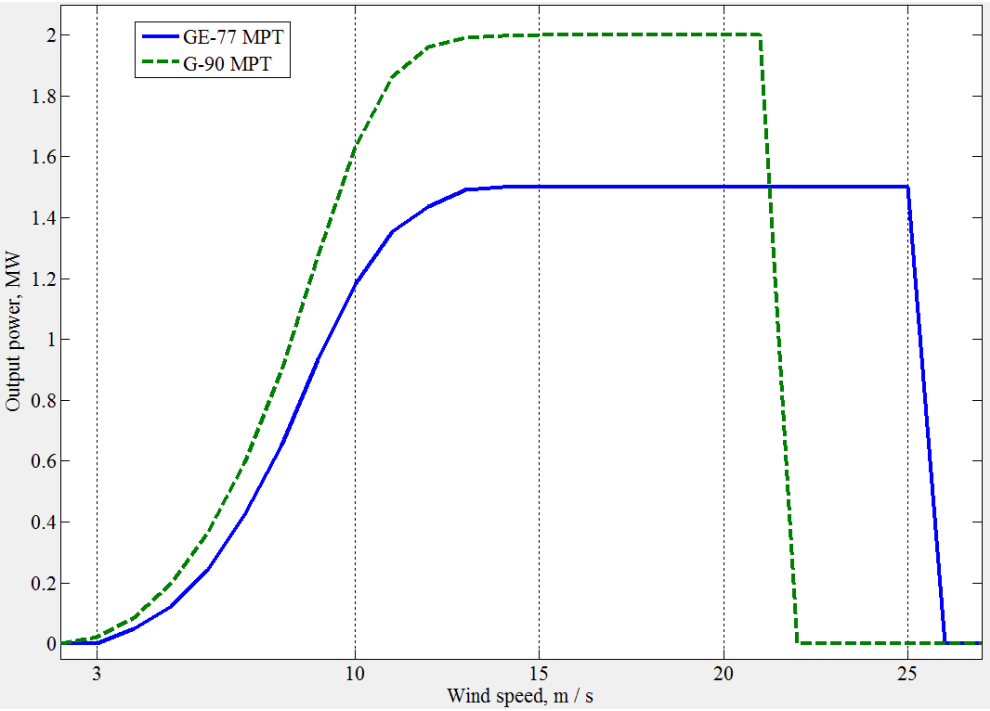

Figure 2. Manufacturer power curves of GE-77 and G-90.

Table 1. Selected locations WS characteristics.

Index	Average	Max.	Cat*. 1	Cat. 2	Cat. 3	Cat. 4	Cat. 5
Nabq	6.9 m/s	18.4 m/s	25.3%	22.5%	15.1%	14.1%	13.3%
Ghareb	9.8 m/s	20.1 m/s	7.1%	7.7%	13.1%	21.2%	21.8%

*: Cat. stands for 'category', and its value is the annual rate of occurrence based on the available WS chronological data (i.e., how many records from the overall 52,560 annual records)

Table 2. WS ranges of each category in m/s.

Cat.	1	2	3	4	5
WS range	$WS \leq 4$	$4 < WS \leq 6$	$6 < WS \leq 8$	$8 < WS \leq 10$	$10 < WS \leq 12$

Table 3. Technical specifications of Integrated WTs types.

WT type	GE-77	G-90
Manufacturer	General Electric	Gameza
Rotor diameter, m	77	90
Hub height, m	80	78
Cut-in WS, m/s	3.5	3
Cut-out WS, m/s	25	21
Default rated WS, m/s	13	16
Nameplate rating, MW	1.5	2
Rotational speed range, radians/s	1.15 -2.51	0.94 -1.99
Optimum tip speed ratio	8.1	10

3. Results and discussion

3.1. Obtained performance curves

First of all, the pivot parameters of the proposed partial de-loading algorithm, clarified in Subsection 2.3, are estimated in the two locations with respect to the two WTs types. There is no big difference between the WTs dimensions and ratings, hence no major deviations in the parameters values as depicted in table (4). For example, the difference in base rotational speed between G-90 and GE-77 is just 0.09 rad/s to the favor of G-90. Likewise, WS_B of G-90 is slower, because it has greater rotor diameter. It is worth mentioning that in Ghareb site pre-analysis showed that, base rotor speed for G-90 should be 2.08 rad/s (the highlighted value in table (4)). However, this *theoretical* value exceeds the maximum allowed speed of G-90, hence the base speed is adjusted to the WT speed ceil, namely, 1.99 rad/s. In particular, the high average WS in Ghareb makes the WTs able to run at high base rotational speed without dissipating energy. On the contrary, WS_B is less compared to Nabq site as the high rotational speed makes the WT reaches P_B at slower WS. For further illustration, the performance curves of GE-77, in case of partial de-loading algorithm, in the considered locations, are shown in figure (3). The breakpoint of Nabq curve is noticed at 12 m/s, because beyond this WS, the rotational speed can increase above its base value without decreasing P_{op}, but it increases. Conversely, breakpoint occurs at slower WS, namely 10 m/s in Ghareb, due to the higher base rotational speed. A comparison between GE-77 and G-90, implementing partial de-loading technique, is depicted in figure (4). It is interesting that, both WTs reach their rated output at almost the same WS, although their default rated WSs deviates by 3 m/s.

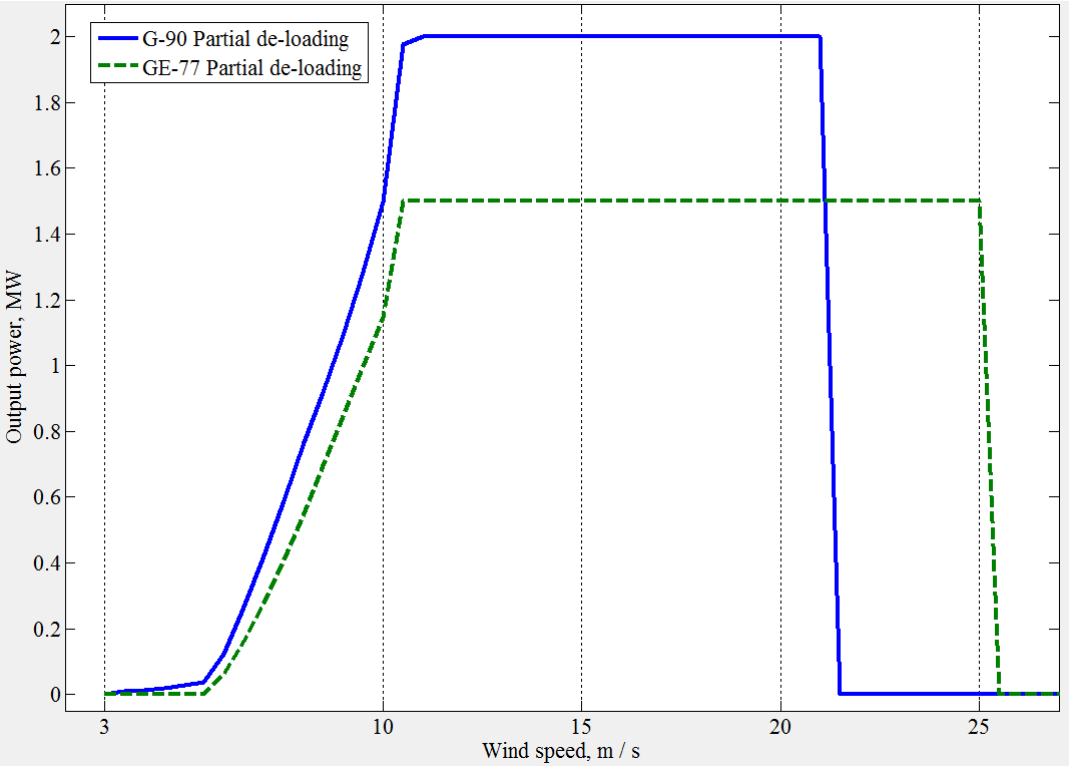

Figure 3. Partial de-loading performance curves for both types in Ghareb site.

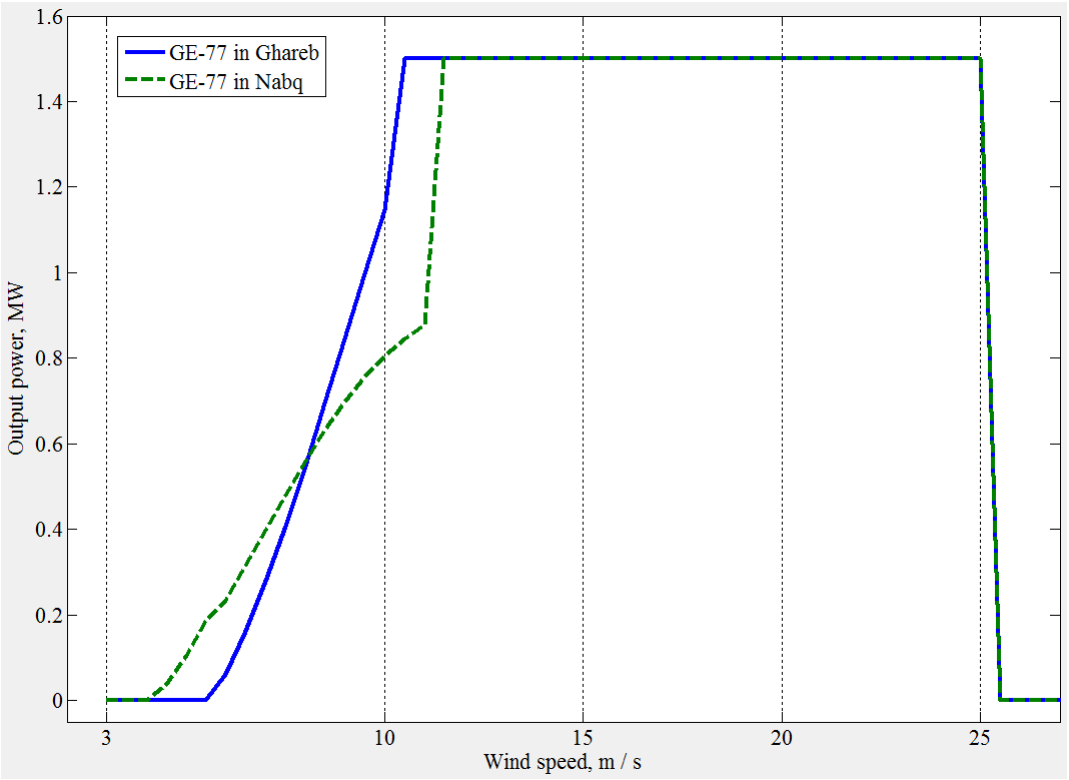

Figure 4. Partial de-loading performance curves for GE-77 in both sites.

For extended clarification, figure (5) displays all G-90 power curves implied in this paper. Firstly, the manufacturer power curve, namely MPT, is compared to the obtained MPT2. The two curves are almost typical except the dissimilarity at the WSs just before the WT reaches rated P_{op}, where in MPT2 curve, P_{op} is higher through this WS range. Likewise, a minor discrimination occurs at relatively low WSs just beyond the $WS_{cut\text{-}in}$. These deviations return to the recording methods applied to determine WT power curve by the manufacturer. In addition, the precise values of aerodynamic model constants have considerable impact on the obtained MPT2 curve.

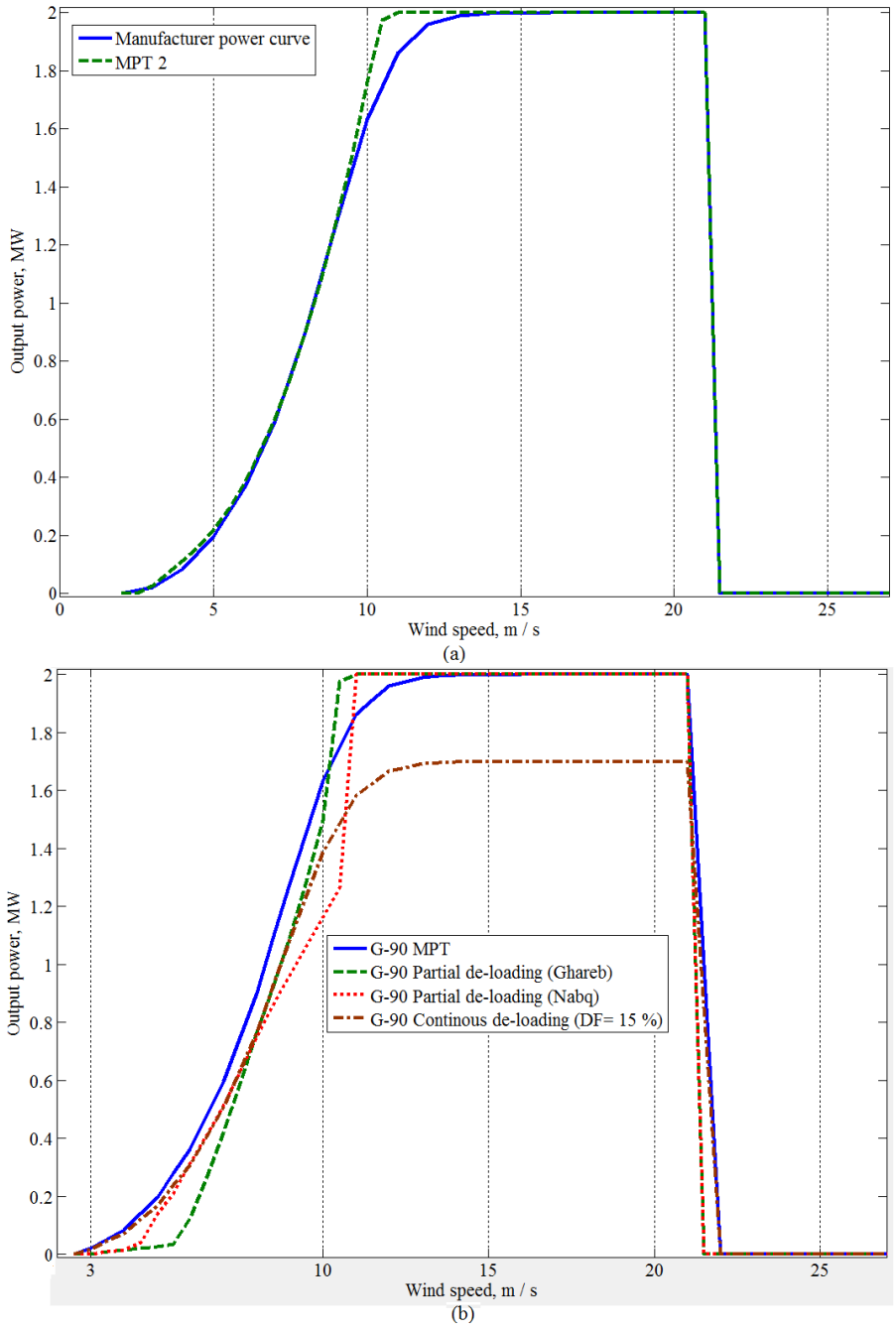

Figure 5. Performance curves for G-90 in all conditions and sites.

Secondly, the breakpoint of Nabq curve lags that of Ghareb. This returns to the low average WS in Nabq location, hence, base rotational speed is slower. Consequently, the WT speed exceeds its base speed without reducing its P_{op} at higher WS. Thirdly, at very low WSs, Nabq curve yields higher P_{op} compared to Ghareb. On the contrary, at medium WSs, Ghareb site has the superiority over Nabq. As an illustration, the de-loaded operation parameters are adapted for low WSs in Nabq due to the lower average WS in this site. Finally, the MPT and the continuous de-loaded curve are typical in attitude. However, the MPT is only rescaled by D_F factor to produce the continually, de-loaded power curve (e.g., the rated output is de-loaded to 1.7 MW in case of G-90).

Table 4. Proposed algorithm parameters in two locations.

Location	Nabq		Ghareb	
WT type	GE-77	G-90	GE-77	G-90
Parameter				
Base rotational speed, rad/s	1.45	1.54	1.96	1.99 (2.08*)
WS_B (m/s) and P_B (p.u.)	10, 0.63	9.5, 0.63	9, 0.66	9, 0.65
WS_{low}, m/s	5.6	5.3	5.04	5.04

*: The value between brackets indicates that, the WT maximum speed limit is violated in the assessment of base rotor speed. Thus, base rotor speed is adjusted to the maximum value.

3.2. Wasted energy analysis

The generated electrical energies through one year, according to the available WS arrays in each location, from one WT in all cases, are gathered in table (5). Achieved results insure that MPT2 curve revealed better operation points for the WT that is why E_{MPT2} is higher than E_{MPT1} in all cases. Nevertheless, the deviations between the two methods fluctuate according to WT type and WS nature in the considered location. In particular, Ghareb has better WS conditions compared to Nabq, hence the impact of the difference between MPT2 and standard power curve increased (i.e., in Nabq E_{MPT2} is higher by 270 MWh compared to 380 MWh in Ghareb). Although the rating of G-90 is more than G-77, but the difference between E_{MPT2} and E_{MPT1}in Ghareb, is higher to the favor of GE-77 by 200 MWh. This could be justified by the accuracy and nature of aerodynamic models of both WTs types.

The implementation of over-speeding technique wastes the lowest amount of energy according to table (5) and figure (6). This merit is achieved by over-speeding technique because: 1) it reduced P_{op} by a small margin, 2) it has a limited activation range ($WS_{cut\text{-}in} < WS < WS_R$), compared to continuous de-loading technique. However, the provided support power from this algorithm is less compared to the other two methods, and it totally depends on the amount of extracted KE. Additionally, this algorithm must decelerate the rotor speed during frequency events, which consumes the electronic converters and increases the risk of loss of synchronism. Moreover, the rotor speed needs to recover its default value after support period, thus P_{op} is reduced until rotor speed satisfies λ_{High} again.

On the other hand, E_{PD} is more than E_D in all cases. In Ghareb site with GE-77 installed, the partial de-loading technique wasted 7.5 %, with respect to E_{MPT2}, compared to 21 % wasted by continuous de-loading method. However, the superiority of partial de-loading is reduced in Nabq because the implied continuous de-loading wasted 21.9 % meanwhile partial de-loading wasted 21.4%. This might be seen trivial, but if the price of kWh based on Egyptian tariff is acknowledged, it means that the single WT wastes annually about 2390 € when it is continuously de-loaded (0.5 % x 4.78 GWh x 0.1 €/kWh). This value is enormously multiplied when the number of WTs in each WF is considered. The results of G-90 emphasize the great losses occurred due to continuous de-loading, as the rating of WT is greater, hence more energy is wasted (keep in mind that, D_F is a percentage from P_{op} not a fixed power amount). For example, in the lower WS site, Nabq, partial de-loading wastes 16 % corresponding to 18.4 % when continuous de-loading is implied in Ghareb. In brief, installing WTs with higher ratings in sites characterized by high WSs, amplifies dramatically the wasted energy by both de-loading techniques. Nevertheless, partial de-loading technique has appreciated merits, and mitigates wasted energy. The aggregation method of the installed WTs in a WF has a considerable impact on the overall harvested energy by the WF. However, the interest of this paper is focused on

the negative influence caused by frequency support algorithms integrated into WT. Therefore, it neutralized the impact of aggregation method by comparing the output of two independent WTs. Moreover, the inclusion of WSs wake and tower effects inside the WF is expected not to cause a great deviation. As an illustration, all the WTs inside a WF should be running by the same algorithm [22]. Hence, the new reduction in WF energy is caused by WS propagation through WF terrain. As an illustration, wake effects and towers shadowing reduce incident WSs on WTs (compared to free stream speed), hence P_{op} of those affected WTs are curtailed. Accordingly, single WT is considered in this research work to neutralize the impacts of WFs dispatching and aggregation that are almost independent from WT operation algorithm.

Table 5. Amounts of annual generated energies (in GWh/year/WT) of each algorithm.

Location	Ghareb					Nabq				
Energy / WT type	E_{MPT1}	E_{MPT2}	E_{PD}	E_D	E_{OS}	E_{MPT1}	E_{MPT2}	E_{PD}	E_D	E_{OS}
GE-77	8.63	9.21	8.5	7.34	9	4.78	5.21	4.09	4.07	5
G-90	11.77	12.15	11.35	10	12	6.63	6.9	5.78	5.63	6.9

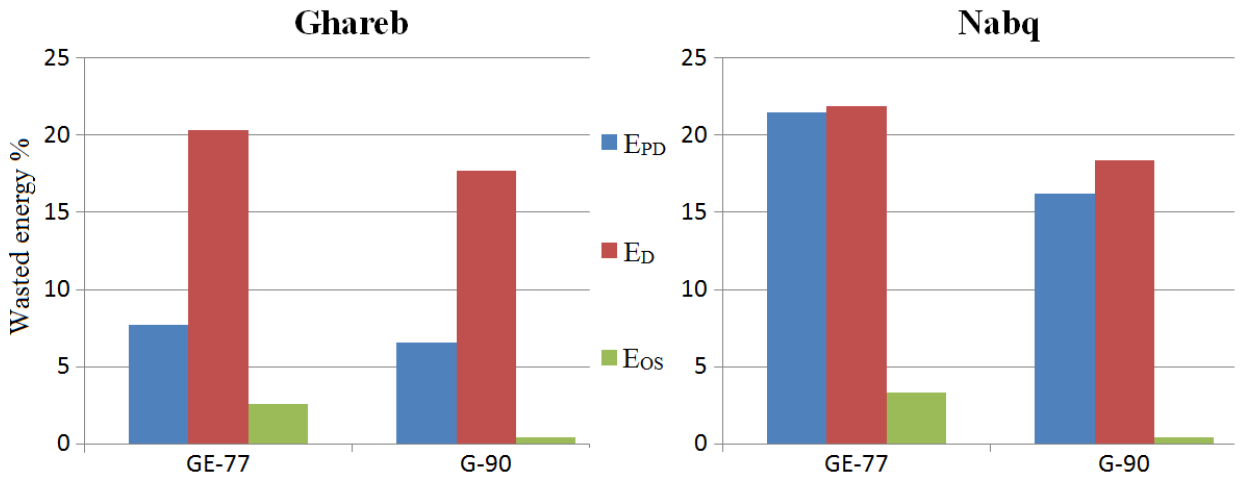

Figure 6. Ratios of wasted energies of all support algorithms compared to MPT 2.

4. Conclusions

The supportive response of WTs during system frequency drops is mandatory at high levels of wind energy contribution in power systems. Particularly, the replacement of conventional power plants with wind farms applies strict requirements from wind farms during voltage and frequency events. In the light of these facts, this paper investigates the major wind turbine operation techniques, including, modified algorithms that secure an acceptable level of power support during frequency drops. The paper has also investigated two different methods to acquire MPT curve and analyzed the differences between the standard method and the proposed one. Two support algorithms count on keeping certain deficit between wind turbine optimum output and the actual generated value (i.e. de-loading operation). Consequently, this deficit acts as a strategic reserve which contributes positively in frequency drops elimination. The third algorithm seeks storing high extractable amounts of kinetic

energy in the rotating parts of wind turbines, so that that this energy is converted into supportive power during frequency events. However, both methods are double edged weapons. Considering de-loading operation; certain amount of wind energy is wasted in normal mode. Additionally, wind turbine deceleration increases the risk of loss of synchronism, besides the recovery period required by the wind turbine to return to its default speed. This paper compared between these support techniques based on the amount of wasted energy, with respect to MPT operation. Results reveal the considerable differences between the two derived MPT curves, and their effect on harvested energy estimation. Outcomes insured the advantage of partial de-loading algorithm in the form of wasted energy reduction, and mitigating fluctuations in rotational speed of wind turbine.

References

1. Holttinen H, Orths AG, Eriksen PB, et al. (2011) Currents of changes. *IEEE Power Energy Magazine* 9(6): 47-59.
2. Kundur P. (1994) Power System Stability and Control. New York: McGraw-Hill Inc.
3. Ekanayake J, Jenkins N (2004) Comparison of the response of doubly fed and fixed-speed induction generator wind turbines to changes in network frequency. *IEEE T Energy Conversion* 19(4): 802-812.
4. Muyeen S, Takahashi R, Murata T, et al. (2009) Low voltage ride through capability enhancement of wind turbine generator system during network disturbance. *IET Renewable Power Generation* 3(1): 65-74.
5. Attya A, Hartkopf T (2013) Control and quantification of kinetic energy released by wind farms during power system frequency drops. *IET Renew Power Generation* 7(3): 210-224.
6. Attya AB, Hartkopf T (2012) Penetration impact of wind farms equipped with frequency variations ride through algorithm on power system frequency response. *INT J Electric Power* 40: 94-103.
7. Attya AB, Hartkopf T (2014) Wind turbine contribution in frequency drop mitigation – Modified operation and estimating released supportive energy. *IET J Generation Transmission and Distribution* 8: 862-872.
8. Rahmat UN, Thiringer T, Karlsson D (2008) Temporary Primary Frequency Control Support by Variable Speed Wind Turbines-Potential and Applications. *IEEE T Power Systems* 23(2): 601-612.
9. Gautam D, Goel L, Ayanar R, et al. (2011) Control Strategy to Mitigate the Impact of Reduced Inertia Due to Doubly Fed Induction Generators on Large Power Systems. *IEEE T Power Systems* 26(1): 214-224.
10. Chang-Chien L, Lin W, Yin Y (2011) Enhancing Frequency Response Control by DFIGs in the High Wind Penetrated Power Systems. *IEEE T Power Systems* 26(2): 710-718.
11. de Almeida R, Peas LJ (2007) Participation of Doubly Fed Induction Wind Generators in System Frequency Regulation. *IEEE T Power Systems* 22(3): 944-950.
12. Le-Ren CC, Yao-Ching Y (2009) Strategies for Operating Wind Power in a Similar Manner of Conventional Power Plant. *IEEE T Energy Conversion* 24(4): 926-934.
13. Margaris ID, Papathanassiou SA, Hatzia ND. (2012) Frequency Control in Autonomous Power Systems with High Wind Power Penetration. *IEEE T Sustainable Energy* 3(2): 189-

199.

14. Martinez J, (2011) Modeling and characterization of energy storage devices. IEEE Power and Energy Society General Meeting; San Diego, CA.
15. Etherden N, Bollen M (2013) Dimensioning of Energy Storage for Increased Integration of Wind Power. *IEEE T Sustainable Energy* 4(3): 546-553.
16. Attya A, Hartkopf T (2012) Evaluation of Wind Turbines Dynamic Model Parameters using Published Manufacturer Product Data. IEEE International Energy Conference and Exhibition; Florence.
17. Ackermann T, (2005) Wind Power in Power Systems; John Wiley & Sons Ltd.
18. Yao D, Choi S, Tseng K, et al. (2012) Determination of Short-Term Power Dispatch Schedule for a Wind Farm Incorporated With Dual-Battery Energy Storage Scheme. *IEEE T Sustainable Energy* 3(1): 74-84.
19. Attya A, Hartkopf T (2013) Wind Energy in Egypt- Capacity Assessment and Analyzing Penetration Impact on Grid Frequency. IEEE 4th International conference on power engineering, energy and electrical drives; Istanbul.
20. Miller N, Price W, Sanchez-Gasca J (2003) Technical Report-Dynamic modeling of GE 1.5 and 3.6 wind turbine-generators; General Electric Company.
21. Mortensen NG, Said US (2009) Wind Atlas for Egypt. New and Renewable Energy Authority; Cairo.
22. Attya AB, Hartkopf T (2013) Wind farms dispatching to manage the activation of frequency support algorithms embedded in connected wind turbines. *INT J Electric Power* 53(1): 923-936.